TD-01-005

VLHC Beam Screen Cooling

C. Darve, P. Bauer, P. Limon, T. Peterson
Fermilab, Technical Division, T&D Department

Keywords: ***VLHC, beam screen, synchrotron radiation and cryogenics.***

1 INTRODUCTION

In the framework of the Very Large Hadron Collider (VLHC) R&D studies, vacuum and beam screen issues are being investigated at Fermilab. This report focuses on the cooling system for the VLHC beam screen and its integration into the VLHC cryo-system. Beam screen cooling is a key issue in the VLHC, due to the large synchrotron radiation (SR) power generated by its intense, high-energy proton beams. Approximate designs of the beam screen are presented to illustrate the space requirements of the beam screen cooling system. The parameters of the high field magnet cooling system are briefly discussed in the context of the beam screen refrigeration. In the cryogenic concept pursued here, the same helium gas will be used to extract the heat loads from the thermal shield of the cryostat and the beam screen. Although the LHC beam screen design serves as a baseline for the calculations presented in the following, new requirements arise with the large synchrotron radiation heat load of ~ 8.5 W/m/beam in VLHC stage 2 (as compared to 0.32 W/m/beam in the LHC).

2 VLHC PARAMETERS

The VLHC machine in its second stage is composed of superconducting magnets operating in supercritical helium at 4.5 K. The magnets generate a 10 T magnetic field, guiding protons of 87.5 TeV around the 240 km circumference ring. According to the current VLHC cryo-concept [1] the magnets will be cooled by 12 cryogenic strings, each 2x20 km long. Seven ~18-m long dipoles and one ~10-m long quadrupole represent a VLHC2 half-cell (~135 m long). The design concept of the VLHC2 cryo-system is presented in further detail in [1]. The beam screen contains the proton beam, absorbing the heat generated by the synchrotron radiation (SR) photons impinging on its inside wall. A preliminary analysis of the space requirement of a beam screen for a former version (2x50 TeV center of mass energy) of VLHC was presented elsewhere [2]. The present note contains the updated calculations for the new VLHC2 parameters. As proposed in [1] a single cryogenic circuit will extract the heat from the thermal shield and the beam screen. The important design parameters for the cryogenic system are the dynamic heat loads (mostly SR) and the static heat loads, scaled from measurements on LHC cryostat thermal models to the VLHC2 system [3-4-5]. Table 1 indicates a higher (10^{35}) and a lower ($2\cdot10^{34}$) luminosity VLHC2 option. The higher luminosity corresponds to an initial design that could not be upheld because of excessive power deposition in the IR's due to the proton-proton collisions. The VLHC2 in its present design would therefore operate at the lower luminosity of $2\cdot10^{34}$. However, the beam screen cooling system calculations were made for the entire range of luminosity and will be presented in their entirety here.

Energy per proton E_b (TeV)	87.5
Peak Luminosity L ($cm^{-2}s^{-1}$)	$2\cdot10^{34}$ (10^{35})
Total Circumference C (km)	241
Bending radius r (km)	29.1
Dipole Field B (T)	10

Circumference Arc l_{arc} (km)	220
Magnet packing factor (%)	85
Number of Bunches N_b	81 106
Initial Nr. of Protons per Bunch $N_{p/b}$	$6.2 \cdot 10^9$ ($1.38 \cdot 10^{10}$)
Bunch Spacing (ns)	9
Revolution frequency f (Hz)	1242
Rms bunch length (cm)	3.3
Number of IP's	2
Beta* (cm)	25
Luminosity life-time (collision loss only) t_L (hours)	9.8 (4.4)
Gamma g	93284
Beam Current I_b (mA)	101 (225)
Radiation damping time t_R (hours)	2.5

Table 1: VLHC2 machine parameters. The high luminosity option is indicated in parentheses.

2.1 SYNCHROTRON RADIATION HEAT LOAD

The synchrotron radiation (SR) is the dominant source of dynamic heat load in the VLHC2. The resistive wall heating heat load and the heat load due to beam loss induced by multipacting (photoelectrons) are believed to be less in the VLHC2 than in the LHC due to the smaller beam current and larger radius of the VLHC2 machine. The combined resistive wall and multipacting heat load is believed to be < 1 W/m/beam. Therefore we considered the beam induced heat load, *Po*, to be equal to the synchrotron radiation heat load P_{SR}. The SR power radiated by the beam can be calculated with the parameters of Table 1 using (1) [6-7], where the power is calculated from the energy loss per proton per revolution ΔE times the number of protons in the ring N_p and the revolution frequency *f*, divided by the sum of the length of all bending magnets. The formula for the energy loss per proton contains the proton rest-mass $m_p c^2$ and the classical proton radius r_p, the Lorentz-factor γ and the bending radius r. The number of protons is calculated from the number of bunches N_b and the number of protons per bunch $N_{p/b}$.

$$p_0 = \frac{\Delta E f N_p}{2\pi r} = \frac{\gamma^4 m_p c^2 4\pi r_p f N_b N_{p/b}}{6\pi r^2} \quad \left(\frac{W}{m}\right) \tag{1}$$

For instance, with a luminosity of 10^{35}cm^{-2}. sec^{-1} the power P_0 (1), is equivalent to 19 W/m per beam, for 2.10^{34}cm^{-2}. sec^{-1}, it is equivalent to 8.5 W/m/beam. This figure becomes smaller (see line 2 in Table 2) if the total radiation power is normalized on the arc length (l_{arc}) instead of $2\pi r$, meaning that the radiation is spread as well over the short straight sections between the magnets, the quadrupoles, etc... Since the lower bounds of the SR are the more realistic numbers, a considerable safety margin is introduced into the design based on the upper bound heat loads. Further SR related calculations are listed in Table 2.

SR power per beam per meter P_{SR} – upper bound (W/m)	8.5 (19)
SR power per beam per meter P_{SR} – lower bound (W/m)	7 (15.5)
Critical energy keV	8.224
# of incident photons per meter (/m-s)	$2.1 \cdot 10^{16}$ ($4.67 \cdot 10^{16}$)
Incidence angle of SR (mrad)	1.31
Spot size of SR due to beam divergence (mm)	0.493
Power deposited on beam screen (kW/m^2)	17.53 (38.68)

Table 2: Synchrotron radiation in the VLHC2. The high luminosity option for VLHC2 is indicated in brackets.

The critical energy in Table 2 is given with:

$$E_{crit} = \frac{3}{2}\frac{ch}{2\pi}\frac{\gamma^3}{r} \quad (J) \tag{2}$$

Half of the power is carried by photons with $E>E_{crit}$. Half of the photons are emitted with an energy larger than 0.08 E_{crit}. The flux of protons in Table 2 is given with:

$$\Gamma = 6.54 \cdot 10^{13} \cdot \frac{I_b(mA)g}{r(m)} \quad \left(\frac{photons}{m-s} \right) \tag{3}$$

The synchrotron radiation in the VLHC2, as with the parameters listed in Table 1 is considerable. (~100 times as much as in the LHC case). The heat load deposited by SR has to be removed by cryogenic refrigeration. The SR converts tightly bound surface molecules into a steadily increasing surface density of physisorbed (weakly adsorbed) molecules of H, C and O. The isotherm density/pressure of e.g. hydrogen increases suddenly as the surface density approaches a mono-layer. Both problems, refrigeration and photo-desorption, can be alleviated by a liner/beam-screen. The liner can be operated at a higher temperature to reduce the cooling power cost. The calculation of the optimal liner temperature is presented in the following.

Fig. 1 shows the power, *Po*, versus luminosity, assuming that the luminosity is varied only through the number of particles per bunch $N_{p/b}$ (see Table 1). The choice of the luminosity will determine the heat load due to the SR. In the current chapter, we analyze the case where no photon stops are used, hence the total load due to the SR must be extracted by the beam screen cooling system.

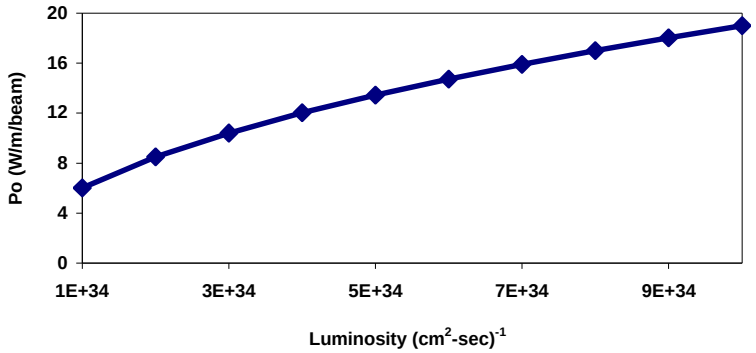

Figure 1: Heat load due to the SR in W/m/beam, *Po*, versus VLHC2 luminosity.

2.2 BEAM SCREEN DIMENSIONS

The beam screen dimensions are dictated by the minimum aperture required for the particle beam and the magnet aperture ("cold bore"). In agreement with first pass VLHC2 beam tracking simulations [8], we made the assumption that the smallest possible beam area is a 10 mm radius circle around the magnet center-line. The coil bore diameter in the common coil VLHC2 dipole is 40 mm, in the VLHC2 arc quadrupole it is 43.5 mm [9]. We assumed that the magnet bore ID is 40 mm. The cold bore is the stainless steel pipe surrounding the beam screen system and inserted into the magnet. It serves as the inner cold mass cryo-vessel wall. A 2x 1.5-mm gap is needed to allow its insertion into the magnet. Then, to withstand the quench-pressure, the cold bore tube needs a minimum wall thickness of 1.5 mm (scaled down from [10]), hence the cold bore inner diameter becomes 34 mm. If we consider the LHC design of the beam screen, we need to foresee beam screen supports. The supports require an additional 2x 0.75-mm gap between the cold bore and the beam screen [11]. Finally, adding up all the gaps and the bore-tube thickness, the remaining aperture (=outer diameter) for the beam screen becomes 32.5 mm. As mentioned before the minimum inner diameter of the beam-screen is determined by the minimum beam area (∅ 20 mm).
Concerning the shape and materials, two main possibilities are under investigation:

1- Stainless steel pipe, copper coated with welded cooling tubes, similar to the LHC approach;
2- Extruded aluminum beam screen system [12];

Sketches of beam screens with designs 1)&2) are shown in chapter 3.
At some magnet interconnections the beam screen cooling tubes need to cross-over to the other aperture to minimize the effect of heat load variations in the 2 beam tubes on the cooling system. In the beam screen

design using steel tubes this is not a problem as long as the ratio of bending radius and tube ID is bigger than 2. In the case of an extruded beam-screen, we could use balancing valves.

2.3 BEAM SCREEN HEAT LOADS AND OPTIMAL TEMPERATURES

The heat load on the beam screen, *Pbs(Tbs)*, can be expressed as a function of the beam screen temperature. It corresponds to the beam induced heat load on the beam screen *Po*, minus the heat load transferred to the cold bore / cold mass. The static heat load on the cold bore / cold mass, *Pcb(Tbs,Tcb)*, emanating from the beam screen depends mainly on the temperature difference between beam screen (*Tbs*) and the cold bore (*Tcb*). Nevertheless, we note that in the case of VLHC2 the heat load induced by the SR, *Po*, will in general be much larger than the heat load transferred to the cold bore, *Pbs*.

$$P_{bs}(T_{bs}) = Po - P_{cb}(T_{bs}, T_{cb}) \tag{4}$$

Heat load to the cold bore

The static heat load on the cold bore *Pcb(Tbs,Tcb)* is coming from conduction through the supports between the beam screen and the cold bore (first term in (5)) and from radiation (second term in (5)).

$$P_{cb}(T_{bs}, T_{cb}) = g\left(T_{bs}^{2.32} - T_{cb}^{2.32}\right) + s\left(T_{bs}^{4} - T_{cb}^{4}\right)\pi d_{cb}\frac{1}{\frac{1}{e(T_{bs})} + \frac{d_{bs}}{d_{cb}}\left(\frac{1}{e(T_{cb})} - 1\right)} \tag{5}$$

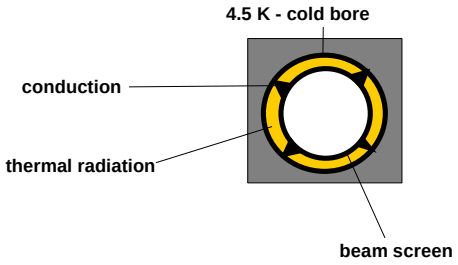

Figure 2: Contributions to *Pcb(Tbs,Tcb)*.

g= thermal conductance coefficients deduced from measurements on the LHC beam screen system with the support-less ("touching") beam screen design = $3.1 \cdot 10^{-6}$ W/m/K$^{2.32}$ [13];
Tbs = beam screen temperature (variable);
Tcb = cold bore temperature (fixed) = 4.5 K;
dcb = cold bore inner diameter = 34 mm;
dbs = beam screen outer diameter = 32.5 mm;
e= emissivity of stainless steel surface(0.1 @ 4 K, 0.2 @ 300 K)
s=Stefan-Boltzmann constant ($5.67 \cdot 10^{-8}$ Watt/m^2/K^4).

At a beam screen temperature of <100 K the radiation between beam screen and beam tube is negligible. Most of the heat transfer between screen and bore occurs through conduction.

Optimum beam screen temperature

The optimum beam temperature can be found by minimizing the total cooling power *Ptot* (6) as a function of beam screen temperature *Tbs* at fixed cold bore temperature (*Tcb*). The Carnot factor *f* (7) assumes a refrigerator efficiency of 0.3. The optimum temperature results in a minimum refrigeration power cost. It balances between the heat load absorbed by the beam screen refrigeration system and the heat load absorbed by the cold mass. At low beam screen temperature the heat load is absorbed mainly by the beam screen, but at low thermodynamic efficiency (7) and thus at high cost. For a beam screen temperature around 100 K, the cost of beam screen refrigeration is reduced, but a significant part of the heat load is transferred from the beam screen by conduction and radiation to the cold mass, where it is again extracted with low thermodynamic efficiency. A first analysis consisted in taking into account only the power to the beam screen and the cold bore. In (6) additional heat loads on the cold bore (resistive heating in the magnet, beam gas scattering, radiation from the shield, conduction through the cold mass supports) were not included, since they do not change the optimum temperature.

$$P_{tot}(T_{bs},T_{cb}) = f(T_{bs})P_{bs}(T_{bs},T_{cb}) + f(T_{cb})P_{cb}(T_{bs},T_{cb}) \quad (6)$$

$$f(T) = \frac{1}{0.3\left(\frac{T}{300-T}\right)} \quad (7)$$

In our model we did not take into account the helium transfer lines (the optimal temperature would be higher in that case) and we did not use over-capacity factors (safety-margins). Figure 3 shows the total plug refrigeration power per meter of beam required to cool one beam screen / cold bore system (neglecting static heat loads on the cold mass emanating from other sources than the beam screen). For a SR heat load of 8.5 W/m per beam, the minimum beam screen cooling power appears to be at 98 K.

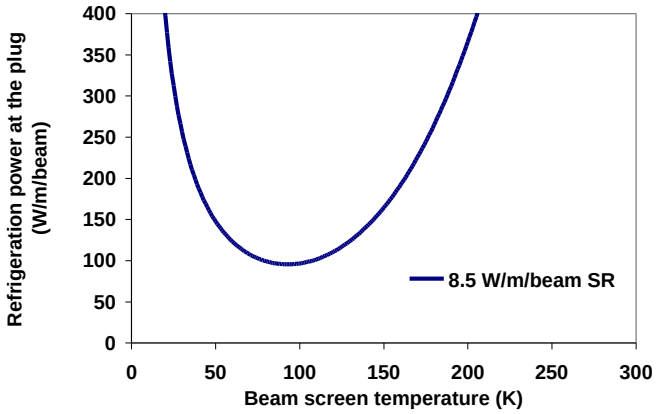

Figure 3: Required refrigeration power (W/m/beam) at the plug to extract a 8.5 W/m/beam SR heat load from the beam-screen/cold mass system (without heat load originating in the cold mass and beam gas scattering power deposition) versus the entry temperature of the beam screen cryogen. Multiply with $2 \cdot l_{arc}$ to obtain P_{tot} for the complete VLHC system.

Since in the cryo-system proposed in [1], the beam screen is operated in series with the thermal shield of the cold mass, we performed our analysis as well for the combined beam-screen / thermal shield system [14]. This computation is in principle similar to the procedure indicated in (5)-(7), except that additional terms for the radiation and conductive heat load on the shield and between the shield and the cold mass are added. In addition the inlet temperature of the beam screen cooling system is fixed by the outlet temperature of the thermal shield system, making the thermal shield inlet temperature the new free variable. If we don't take into account the beam screen but we consider the thermal shield alone, the optimal temperature of the thermal shield is 64 K. This is comparable to the LHC thermal shield temperature, where the contribution of the beam screen heat load to the cooling scheme is indeed negligible (low SR). The computation of the total (thermal shield and beam screen combined) refrigeration power, yields obtain an optimum thermal shield temperature of 94 K, which automatically results in 106 K for the average beam screen temperature. The minimal total refrigeration power of 2 screens, the cold mass and the shield combined (excluding transfer lines and safety factors) would correspond to 6.2 MW for 20 km (309 W/m).
A beam screen operating at 76 K (inlet temperature of the thermal shield equal to 60.42 K), as proposed in [1], is very close to the optimum case for a negligible SR heat load as in the LHC. In the VLHC2 with 8.5 W/m/beam it would result in an increase of about 15 % of the total refrigeration cost compared to the optimum case. On the other hand, as shown in Figure 4, the optimum beam screen temperature quickly drops as the SR heat load is reduced. The increase in refrigeration power cost is only of 4 % in such a case (76 K thermal shield inlet temperature) for a SR heat load of 4 W/m/beam.

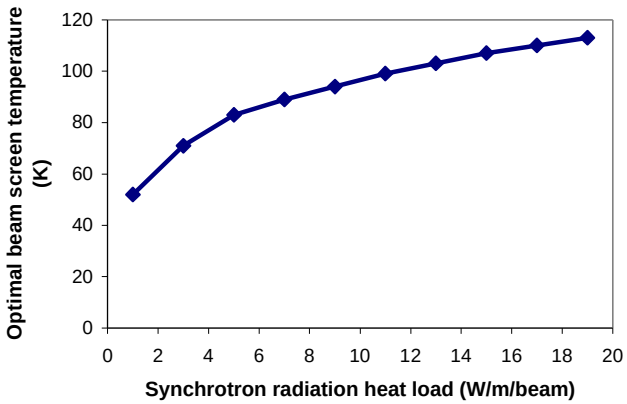

Figure 4: Optimal Beam screen temperature for a given (SR) heat load on the beam screen.

3 BEAM SCREEN COOLING SCENARIOS

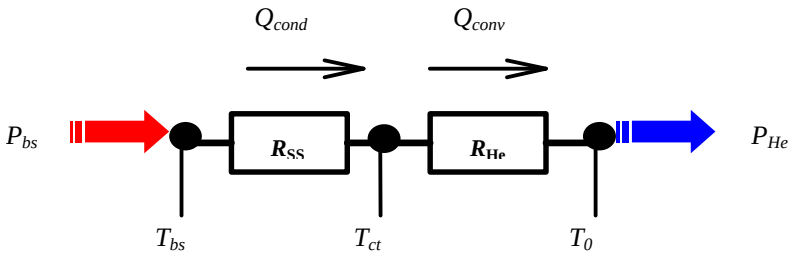

Figure 5: Simplified thermal network model for the beam screen cooling: The incoming heating power P_{bs} is conducted through the steel path (R_{SS}), transferred into the helium through forced convection (R_{He}) and finally transported in the helium P_{He}. The key temperatures along the path are T_{bs}, the beam screen temperature, T_{ct}, the inner wall temperature of the cooling tube (and approximately the radial peak temperature of the helium) and T_0 the average helium temperature in the beam screen cooling loop.

To simulate a possible cooling scenario we sought a solution to the set of equations mentioned below: a continuity equation for the heat flux from the spot hit by radiation to the cooling system (11) and a global energy balance equation (12). The path of the heat flux is illustrated in Figure 5. The heat flux equation demands that the heat flux from the hot spot on the beam screen to the cooling tube Q_{cond} and the flux being transferred into the helium Q_{conv} are equal and consistent with the initial heat flux P_{bs}=Po.
The conductive heat transfer in the beam screen is given in (8), where k is the integrated thermal conductivity of the chosen material (e.g. stainless steel or aluminum), S the cross-sectional area per unit length across which the heat is transported (i.e. the contact area between the beam screen and the cooling tube), L the length of the beam screen cooling system and l the length of the heat path.

$$Q_{cond} = \frac{S}{lL}\int_{T_{ct}}^{T_{bs}} k(T)dT \qquad \left(\frac{W}{m}\right) \tag{8}$$

The cooling heat transfer-correlation is of the forced convection type (9) – with the helium in the supercritical state. It is assumed that the flow is turbulent. The average helium temperature T_0 and the peak temperature (assumed to be the wall temperature T_{ct}) are variables. A_{ct} is the inner cooling duct wall surface over the full length L of the cooling system, the heat transfer coefficient h (10) is calculated from the Nusselt-number at the average helium temperature, the helium heat conductivity k and the diameter of the cooling duct d_{ct}.

$$Q_{conv} = \frac{A_{ct}}{L} h(T_0)(T_{ct} - T_0) \qquad \left(\frac{W}{m}\right) \tag{9}$$

$$h(T_0) = Nu \frac{k(T_0)}{d_{ct}} \quad \left(\frac{W}{m^2 K}\right) \tag{10}$$

$$Q_{conv}(T_{ct}) = Q_{cond}(T_{ct}) = p_{bs} \quad \left(\frac{W}{m}\right) \tag{11}$$

The energy balance equation (12) states that the heat deposit on the beam screen is at least equal to the heat removal capacity of the helium. The heat removal capacity of the helium is calculated from the mass flow rate *dm/dt*, the temperature difference over the full length of the cryogenic system T_{out}-T_{in}, and the specific heat c_p, taken at the average longitudinal helium temperature in the system (T_0).

$$p_{He} = \frac{dm}{dt} c_p(T_0)(T_{out} - T_{in}) \frac{1}{L} \qquad \left(\frac{W}{m}\right) \tag{12}$$

The solution is found iteratively from a first guess of A_{ct}, *dm/dt*, T_{out}, T_{in}, T_{ct} *and* T_{bs}.
Calculations using integrated material properties for the convective heat transfer for the temperature interval (T_{in}, T_{out}) instead of an average temperature in the helium did not give any different results!

Various scenarios were considered for the beam screen cooling. A high cryogen pressure is required in the case of SR heat loads exceeding ~1 W/m/beam. The high pressure requirement is partly related to the higher beam-screen temperatures (reduced cryogen density) and to the high mass flow requirements which result in high pressure loss in the system. Then, only helium was pursued because of safety issues with nitrogen [9]. Therefore the working assumption was a high pressure (20 bar) helium circuit – 135 or 270 m long. The goal was to minimize the refrigeration power. The following limitations were as well considered:

- The pressure drop between the front and rear section of the beam screen cooling loop was kept below 1 bar in order to operate the compressors with optimal efficiency.
- We characterize the available cross-section area for the beam screen cooling ducts as a percentage of the cross-sectional area enclosed by the cold bore (∅ 34 mm). The minimum beam area (∅ 20 mm) represents 40 % of the surface. The missing 32 % are reserved for the wall thickness of the beam screen, the walls of the cooling duct(s) and "un-used" surfaces. Hence, the cooling cross-section was limited to 28 % (14 tubes of 5.3 mm welded around a 20 mm outer diameter beam screen).
- The length of the half-cell is important to estimate the pressure and temperature drops: 135 m (half-cell) and 270 m (cell) long sections were considered in our simulations.

The solution outlined in the following plots (Figure 6 and Figure7) is the baseline_100 K solution, i.e. the chosen solution with an optimal beam screen temperature of 100 K at a SR heat flux of 8.5 W/m/beam (VLHC2 luminosity = 2.10^{34} $sec^{-1}.cm^{-2}$). Figure shows the calculated pressure drop as a function of the cooling tube cross-sectional surface (i.e. the required cross-sectional area of cryogen). The calculation was performed for a beam screen cooling tube length of 135 m (half-cell). Three curves are shown, representing several possible temperature differences between the entrance and the exit of the beam screen cooling system: 21 K, 30 K and 44 K. The two lines in the plot outline the area of possible Δp/surface combinations (Δp< 1bar and cross-section area< 28 % of the cold bore cross section). shows the mass-flow requirement versus SR heat load for a beam screen with a 16.16 % cooling cross-section (100 %= cold bore inner cross-section) and temperature 100 K. The line indicates the maximum allowable mass-flow for state of the art cryogenic systems. Figure 6 and Figure7 represent solutions that can be implemented in a cryogenic system. The working points outlined in the figures refers to the baseline scenario case 1 in the following table (Table 3).

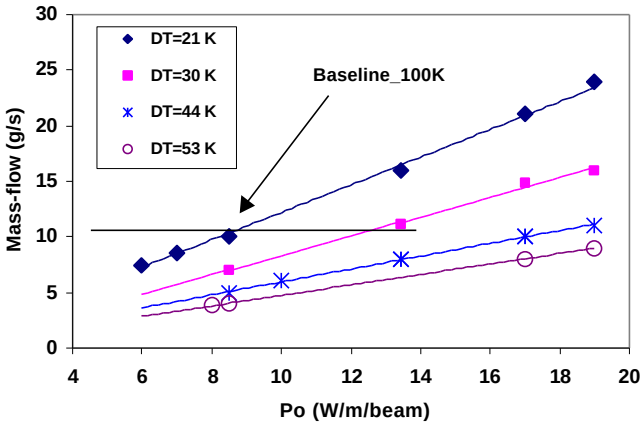

Figure 6: Mass-flow needed versus the heat load due to synchrotron radiation, *Po*. The cooling section is 16 % of the cold bore inner section, and the cell length is 135 m.

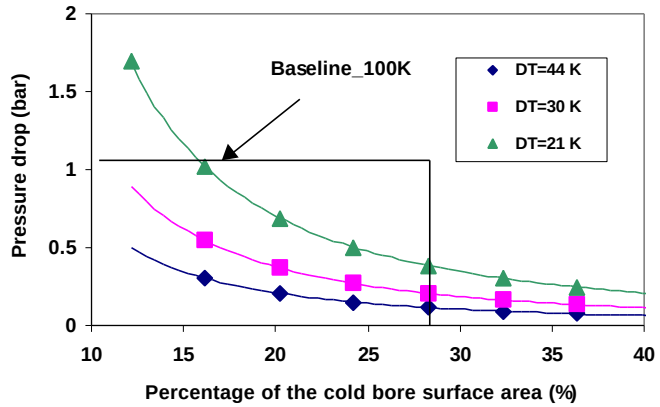

Figure 7: Pressure drop calculated for various conditions, *Po*=8.5 W/m/beam. Beam screen temperature T_{bs}=100 K. The mass-flow are 5 g/s, 7 g/s, 10 g/s for the temperature drop 44 K, 30 K, 21 K, respectively. The pressure drop and the temperature increase are calculated over a system length of 135 m.

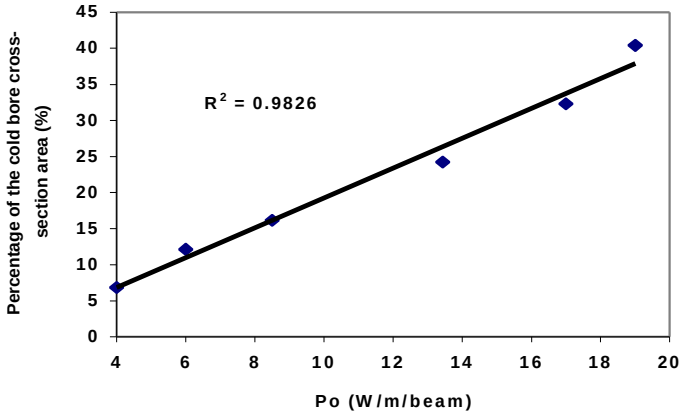

Figure 8: Percentage of the cross-sectional area of the cold bore to be filled with cryogen versus the heat load generated by synchrotron radiation *Po* (in % of the surface enclosed by the cold bore – ∅ 34 mm). Pressure drop ~ 1 bar, temperature drop 21 K, half-cell length (135 m).

Table 3 presents solutions for 5 possible cases:

1) Case 1, the base-line case, assumes a 8.5 W/m/beam SR power (as given for a $2{\cdot}10^{34}$ luminosity) and an average (non-optimal) beam screen temperature of 76 K as proposed in the VLHC cryo-concept [1]. The solution requires a considerable 16.2 % of cryogen cross-section in the cold bore, a large mass-flow rate of 11 g/s and is feasible only for a loop over a half-cell if the temperature drop along the beam screen cooling system is to be kept <20 K.
2) Case 2, "the ideal case" (or Baseline_100K) from the beam screen point of view, i.e. operating at the optimum beam screen temperature, assumes a 8.5W/m/beam SR load (as given for a $2{\cdot}10^{34}$ luminosity) and a half cell loop. The solution is similar to case 1, except for a lower mass flow rate of 10 g/s (meaning a lower helium inventory).
3) Case 3, assumes a 8.5 W/m/beam SR load (as given for a $2{\cdot}10^{34}$ luminosity) with 4 W/m/beam being absorbed in the photon stops! The mass-flow rate can be drastically reduced (compared to case 1) to 4.5 g/s. In the case of a stand-alone beam screen system, operated at the temperature of 76 K, the cryogen cross-sectional area could be reduced down to 7% of the cold bore cross-sectional area. It has to be noted that the solution presented here was found for an independent beam-screen. In a cooling scheme, where the beam screen is combined with the thermal shield, the optimal thermal shield temperature becomes 80 K (beam screen optimal temperature=106 K).
4) Case 4, corresponds to case 2, except that the cooling loop was made a full cell length. The mass flow rate has to be reduced to keep the pressure drop below 1 bar and the temperature difference between entry and exit increases significantly!
5) Case 5 represents a solution for the 10^{35} luminosity VLHC2 design. The cryogen would take up 24.4 % of the cross-section. The flow rate is very high – 14 g/s. The temperature difference is 35.5 K. Case 5 is presented to show that even such an extreme heat load as 19 W/m/beam can be extracted from the beam screen at the considerable sacrifice of a large part of the magnet aperture for beam screen cooling!

	Case 1 Baseline	Case 2 Bl_100K	Case 3	Case 4	Case 5	LHC
Luminosity($cm^{-2}.sec^{-1}$)	2.10^{34}	2.10^{34}	2.10^{34} + photon stop	2.10^{34}	10^{35}	-
Average beam screen T (K)	76	100	76	100	100	14
***Po* / SR heat load (W/m/beam)**	8.5	8.5	4	8.5	19	1
System length (m)	135	135	135	270	135	250
Total mass-flow per beam screen (g/s)	11	10	4.5	4	14	1.1
T. @ inlet of the beam screen (K)	65.3	89.5	72.7	73.4	82.2	5
Cross-section (% of cold bore)	16.2	16.2	7.4	20.2	24.4	2.1
Pressure drop (atm)	0.88	1.02	1.1	0.93	0.90	0.13
T. @ outlet of the beam screen (K)	84.8	110.4	92.0	126.6	117.7	20
Temperature difference (K)	19.5	20.9	19.3	53.2	35.5	15

Table 3: Different beam screen cooling scenarios. All data refer to one beam. LHC data are shown in the last column.

Figure 9: Section of stainless steel (left) and extruded Al (right) beam screen. The number of tubes in the LHC type beam screen, and the indicated cryogen quantity in the extruded type beam screen, represent the baseline (case 1) beam screen cooling system in Table 3.

The previous sketches (Figure 9) are not intended to represent serious beam screen designs. They solely serve the purpose of illustrating the basic beam screen dimensions and proportions of the cross sectional area reserved for the cryogen. The outer diameter of the beam screens in the sketch is 32.5 mm. In the case of the LHC type beam screen, the cold bore tube is outlined as well. Figure 9 shows a sketch of an extruded aluminum beam screen. The pockets carry the cryogen. In Figure 9 two pockets are filled, which corresponds to the cooling requirements for the baseline solution presented here (case 1,2). The high luminosity case would require all 4 pockets to be filled. The case in which photon stops absorb half of the 8.5 W/m/beam synchrotron radiation, only one pocket would be filled. The right and left channels are used to extract the heat loads mainly due to the synchrotron radiation (SR). The left sketch represents an LHC type solution applied to cases 1&2: 8 cooling tubes are required to cool the beam screen. The inner diameter of the tubes would be 5.3 mm. The wall thickness is 0.5 mm.

4 MISCELLANEOUS

4.1 PHOTON STOPS

A possible use of a photon stops would permit a reduction of the synchrotron radiation heat load on the beam screen [7]. The devices would remove heat at singular points between the magnets, operating at room temperature. This can help considerably in reducing the overall cost of the VLHC cryogenic system. Case 3 in Table 3, presents a scenario in which the photon stops scrape off ~50 % of the 8.5 W/m SR heat load.

4.2 BEAM SCREEN AT ROOM TEMPERATURE

Another solution was envisaged with a beam screen operating at room temperature. The drawback of this solution is the need of a thermal shield between the beam-screen and the cold bore. The idea is to remove the residual heat from this shield (~3.6 W/m) by using a common cryogenic circuit for the thermal shield described previously and the beam screen shield.
Figure 10 shows the comparison between the two solutions: solution 1, described in the previous chapter with a 100 K beam screen and solution 2 with the beam screen at room temperature. For this second solution, a thermal shield reduces the heat load from the beam screen to the cold bore. This beam screen thermal shield is in series with the cryostat thermal shield. The results are relative to a 22 mm inner diameter beam screen thermal shield, with an emissivity equivalent to that of electrolitically polished aluminum. As an assumption we used the same thermal conductance coefficients for the solid conduction from the room temperature beam screen to the shield and from the shield to the cold bore. This value is taken from measurements on the LHC beam screen system with the support-less beam screen design (see γ in equation (5)).

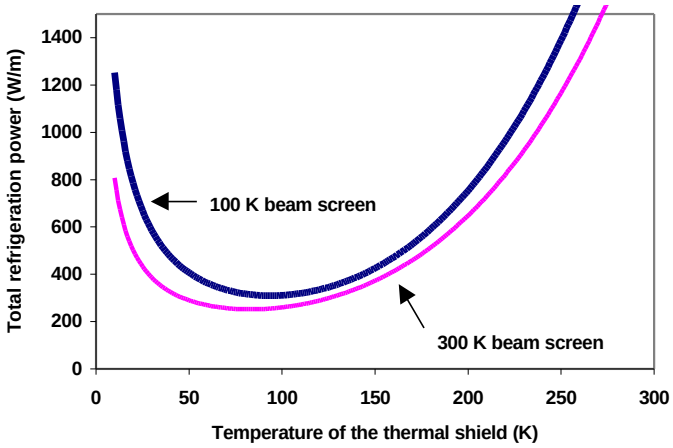

Figure 10: Comparison of the total refrigeration power for the 100 K and the 300 K beam screen systems.

For solution 2, the optimal temperature of the thermal shield becomes 83 K. Then, the beam screen thermal shield is 95 K. Results show that a reduction of the total refrigeration cost by 23 % could be achieved with the 300 K beam screen instead of the 100 K beam screen (that is a saving of 1.15 MW per 20 km string).
However, the problem with the 300 K beam screen is the space requirement: the "inner" thermal shield cooling system, the beam screen room temperature cooling system and some insulation between the thermal shield and the cold bore (not included in the given calculations) is much larger than the space a 76-100 K beam screen system (e.g. cases 1,2,3 in Table 3) would require. A total of 6 tubes - ID 5.3 mm, wall thickness 0.5 mm - are required for the inner shield cooling (20 % of the cold bore cross-section area, including the cooling tube walls). Additionally one tube is required for the 300 K beam screen cooling system (3 % including the walls). The beam screen wall - ID=18.5 mm, OD=22 mm, wall thickness 1 mm, support gap 2 x 0.75 mm - represents 12 % of the cold bore cross-section area (including support), the thermal shield walls – ID=22 mm, OD=25.5 mm, support gap: 2x 0.75 mm - 14.4 %. The sum of all these areas represents 40 % of the cold bore cross-section. This calculation does not include any un-utilized space. If one includes the un-utilized space and the 40 % minimum space requirement for the beam area the magnet aperture can be considered as maximally filled. An additional resistive layer (e.g. 1mm) between the beam screen thermal shield and the cold bore (such a resistive layer was not included in the thermal calculations presented above) requires an additional ~20 % of the cold bore surface. This extra layer would certainly not fit into a magnet aperture of 40 mm! An increase of magnet aperture is certainly more expensive than the above mentioned savings on the cryogenic operations budget. In addition the thermal shield would interfere with the "natural" cryopump function on which the LHC and VLHC vacuum systems currently rely. Another, perhaps more expensive and space consuming form of distributed pumping would have to be packed into the magnet aperture! We therefore believe that the room temperature beam screen solution is not compatible with a 40 mm magnet aperture.

4.3 MATERIAL ISSUES

LHC beam screen supporting system

The LHC beam screen supports are bi-metallic rings (0.25 mm thick stainless steel layer, co-laminated with an outer 0.15 mm CuSn layer to reduce friction with cold bore cross-section), 4.5 mm wide welded onto the beam screen every 500 +/- 50 mm.

LHC Beam screen cooling tubes

The cooling tube inner diameter is 3.7 mm, its wall thickness is 0.53 mm. The cooling tube is made from a specially developed high manganese and high nitrogen content stainless steel grade (P506, Boehler) with a magnetic permeability of <1.005 (at T~5-20 K).

5 CONCLUSIONS

The design of the VLHC high field beam screen within a 40 mm magnet aperture is feasible although constraints are stringent and surfaces important. The current status of the VLHC2 beam screen cooling issue is:

- Several solutions for the beam screen cooling problem in the VLHC2 were proposed. These solutions are applicable to extruded aluminum beam tubes as well as LHC-type beam screens.
- The current VLHC cryo-system design [1] has been analyzed: the use of a beam screen at 76 K and a thermal shield at 60 K increases the cost of SR heat load extraction by 15 % compared to optimal conditions (both thermal shield and beam screen at about 100 K). On the other hand, the use of photon stops and thus the reduction of the SR power to be extracted at low temperature, shifts the thermodynamic optimum towards the chosen 76 K beam screen temperature.
- The solution proposed in the current VLHC cryo-concept [1] (for the total 8.5 W/m/beam SR load) requires a cross-section equal to 16 % of the cold bore cross sectional area for the cooling channel. The total mass-flow rate per beam tube is ~11 g/s. The temperature drop over a half-cell is ~20 K. The pressure drop at an operating pressure of 20 bar is ~1 bar.
- The operation of a beam screen at room temperature would permit to save up to 23 % of the total refrigeration cost. However, this solution would require larger magnet apertures.

More vacuum technology and material issues need to be investigated in view of a final beam screen design. Still, the study of the beam screen cooling issue has revealed several limitations!

References

[1] T. Peterson, P. Bauer, C. Darve, R. Rabehl, “VLHC-2 (High Field) Cryogenic System Concept”, Fermilab, Technical Division Note, still in draft stage 02/2001.
[2] C. Darve, P. Bauer, B. Jenninger, T. Peterson, “Very Large Hadron Collider Beam Screen Design – Preliminary Investigation of Space Requirements”, VLHCPUB 92, 06/1999.
[3] C. Darve, G. Ferlin, M. Gautier, L.R, Williams, “CTM3, the latest evolution of the cryostat thermal model: thermal performance measurements of the first run from March to May 1998”, LHC-CRI Technical Note 98-19, 03/1999.
[4] C. Darve, G. Ferlin, M. Gautier, L.R, Williams, “Thermal performance measurements for a 10 meter LHC dipole prototype (Cryostat Thermal Model 2)”, LHC-Project-Note-112, 11/1997.
[5] L. Tavian, U. Wagner, “LHC sector heat loads and their conversion to the LHC refrigerator capacities”, LHC Project Note 140, 05/1998
[6] H. Wiedemann, “Bending Magnet Radiation”, p. 183 of the Handbook of Accelerator Physics and Engineering, A.W. Chao, M. Tigner, editors, World Scientific 1999.
[7] I. Terechkine, “Synchrotron Radiation Issues for the 87.5 TeV proton beam”, Fermilab, Technical Division Note, still in draft stage, 01/2001.
[8] S.Peggs, Presentation at the VLHC workshop meeting, Fermilab, 01/12/2001.
[9] V. Kashikin, A. Zlobin, “Magnetic Designs of Fermilab 2 in 1 Nb3Sn Dipole Magnets for VLHC”, Proceedings of the Applied Superconductivity Conference, Virginia Beach, Sept. 2000;
[10] S. Yadav, M. Lamm and J. Kerby, “Design Calculations for the LHC IR Quadrupole Magnet Beam Tubes”, TD-99-072, 12/1999.
[11] P. Cruikshank et.al , “Mechanical design Aspects of the LHC Beam Screen”, LHC Project Report 128, 07/1997
[12] W. Chou, “Feasibility Study of Using Aluminum Alloy for the LHC Beam Screen”, LHC Project Note 3 (SL/AP), 08/1995
[13] D. Bozzini, P. Cruikshank, C. Darve, B. Jenninger, N. Kos, D. Willems, “Heat Flow Measurements on Beam Screens with and without Supports”, LHC-Project-Note-200, 09/1999.
[14] C. Darve, “Optimum temperatures for the VLHC thermal shield”, TD-01-XXX, 03/2001.